HIERARCHICAL SIGNAL FUSION NETWORK FOR PULSAR DETECTION WITH PHASE-CORRELATION AND SIGNAL ATTENTIONS

*Huajian Wu and Mingmin Chi**

School of Computer Science, Shanghai Key Laboratory of Data Science, Fudan University, China

ABSTRACT

The discovery of pulsars is of great importance to human understanding of the universe. Deep learning has exploited to find pulsars based on radio astronomical folded data, which includes time-phase and frequency-phase images and dispersion curve (DM). In this paper, a hierarchical signal fusion network with phase-correlation and signal attentions are proposed. Specially, signal attentions are designed to reinforce the pulse signals of time-phase or frequency-phase images if a pulsar appears. After that, pulse signal can be reinforced in the same phase where pulses exist in both images. Accordingly, the pulsar search network is implemented by hierarchical data fusion. The first layer is performed at the feature level through phase correlation attention. The second layer of data fusion done at the decision level is performed by calculating a mapping function weighted by the values provided by the phase-correlation attention and filtered out by the DM peak features for the final discrimination . The proposed model is validated on the FAST public dataset with a significant improvement in recall and AUC compared to existing single and multimodal deep models with different attentions.

***Index Terms*—** Correlation attention, Coupled deep fusion network, Mutimodal data, Pulsar detection, Signal attention

1. INTRODUCTION

Pulsar detection has been taken to manually design statistical features using shallow machine learning methods [1, 2, 3, 4, 5] based on folded signals including profile and dispersion curve (DM) as shown in Fig. 1. Later, deep learning has been utilized for the task [6, 7, 8, 9, 10, 11, 12, 13] based on time-phase (subint) and frequency-phase (subband) images, profile, and/or DM signals. In the existing methods, the multimodal data are integrated in a decision level, which has not considered the correlation between different modal signals.

If a pulsar is present, time-phase, frequency-phase images, or DM curves, will have pulses or peaks present. Thus, how to effectively determine the pulses or peaks is one of the key issues. In addition, if there is a pulse, the time-phase and frequency-phase images will have pulses in the same phase.

Based on this premise, we propose a hierarchical signal fusion network with signal attentions to enhance the characteristics of pulses or peaks and also a phase-associated attention is designed to reinforce the peaks in the same phase. Furthermore, the deep fusion network is implemented in a hierarchical manner. The first-level data fusion is performed at the feature mode through phase-correlation attention, and pulses based on subint and subband images in the same phase are enhanced if pulses are present. Since the presence of peaks in the DM curve is necessary to determine the presence of pulses, the second-level data fusion is performed by calculating a mapping function weighted by the values provided by the phase-correlation attention and the DM signal attention for the final discrimination. The proposed model was validated on the FAST public dataset with a significant improvement in recall and accuracy compared to existing methods.

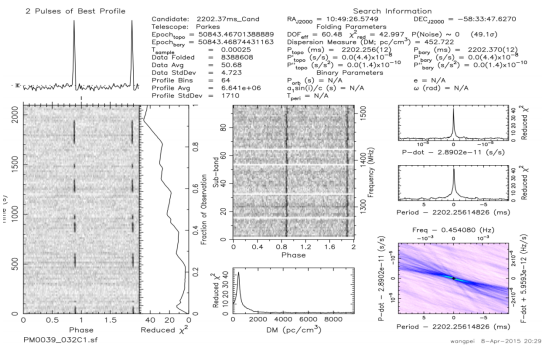

Fig. 1. **Pulsar signal candidate diagram.** After the original astronomical signal is preprocessed[14], a frequency-time-phase signal and a dispersion curve (DM) are obtained, and then the time-phase image (subint) at the lower left is obtained by integrating over frequency, and the frequency-phase image (subband) at the upper middle is obtained by integrating over time. Generally, when a pulsar signal appears, there is a distinct signal on both subint and subband, and there is the presence of some shape of peak on DM.

*Mingmin Chi (mmchi@fudan.edu.cn) is the corresponding author. This work was supported in part by Natural Science Foundation of China under contract 62171139 and by the science and technology development project provided by Tencent Youtu Lab.

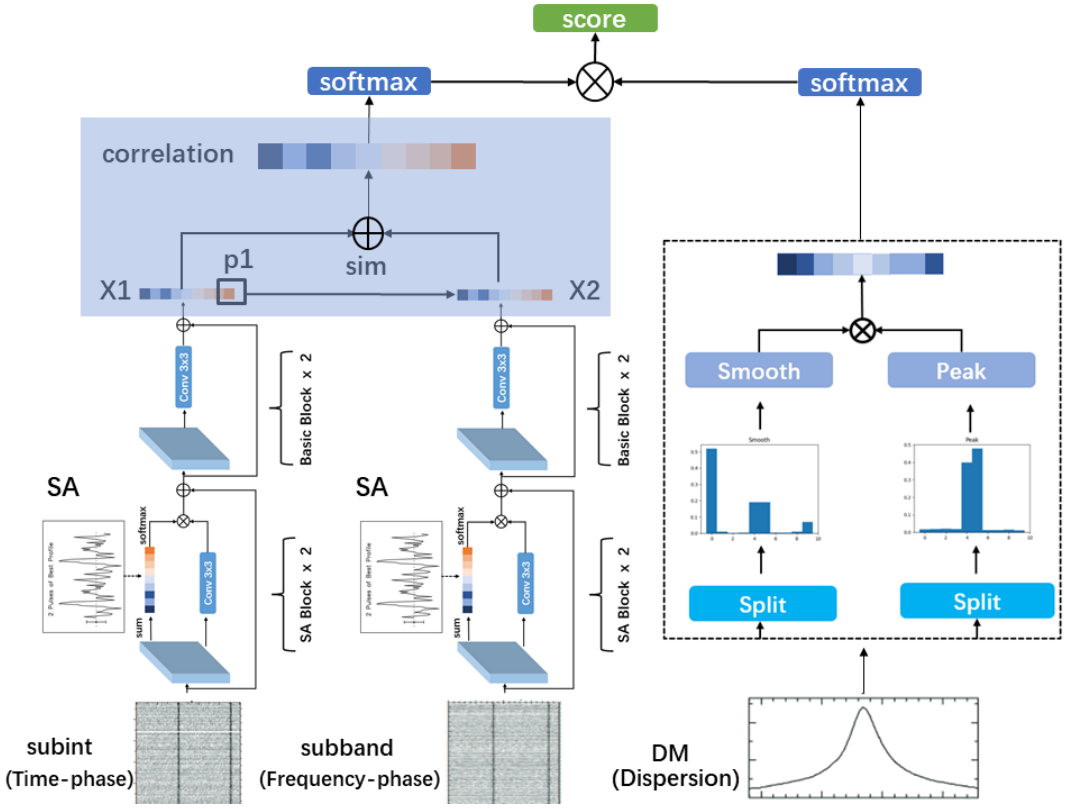

Fig. 2. **Overall architecture of hierarchical signal fusion network.** Through phase-correlation attention, the first-level fusion is performed to enhance the pulse signals for subint and subband images in the same phase if the pulses are present. Since the presence of peaks in the DM curve is necessary to determine the presence of pulses, the second-level fusion first filters out the non-pulse signals and then a mapping function weighted by the values provided by the phase-correlation attention is calculated for final pulsar detection.

2. HIERARCHICAL SIGNAL FUSION NETWORK

In recent decades, radio signals are usually transformed by fast Fourier transform and subjected to a dispersion operation to align the received electromagnetic signals of different frequencies. Afterwards, the period and dispersion values can be obtained. To eliminate interference noise, the observed pulse signals are period superimposed to enhance the pulse signal. Accordingly, we can obtain the time-phase or frequency-phase diagram as well as dispersion curve as shown in Fig. 1. Based on this we can judge pulsars by visual observation or by statistical or machine learning models.

To detect a pulsar signal, the "pulse" features of the subband and subint images should be extracted and reinforced for a better pulsar discrimination, which will be implemented by signal attention as shown in the left part of Fig. 2. In order to reduce the false alarm rate of pulse features, the features that have pulses on both the subband and subint diagrams at the same phase value are mutually reinforced, and thus a phase correlation attention module is added to the deep pulse fusion network.

Since the presence of peaks in the DM curve is necessary to determine the presence of pulsars, "peak" features should first be extracted from the DM curve to filter out non-pulsar signals, which will be combined with the decision function of the subnetwork learned through subband and subint images for final pulsar discrimination to improve the recall of pulsar identification, as shown in the right part of Fig. 2.

2.1. Signal attention for time-phase and frequency-phase images

The presence of pulse signals on the time-phase or frequency-phase images is a key indicator for determining whether a signal is a pulsar.

Thus, how to effectively extract this pulse information is the key to feature extraction based on time-phase or frequency-phase maps.The SA block is obtained by adding the signal attention to the Basic Block of Resnet, and we obtain the enhanced signal characteristics by dot-multiplying the signal intensity distribution on the phase with the vector obtained after convolution.

Signal attention needs to assign relatively high attention weights to the phases where the signal is strong. Therefore, first we need to obtain the intensity distribution of the signal by

$$saf(X) = f(\Phi_{sum}(\Phi_{norm}(X))), \quad (1)$$

where Φ_{norm} refers to the normalized preprocessing of the whole time-phase or frequency-phase signal, Φ_{sum} refers to the summation of the time-phase features in time or the summation of the frequency-phase features in frequency to obtain the signal intensity in different phases, and f refers to the softmax normalization function. Finally, it is normalized to obtain the attention weights for each phase. In addition, we compare various network structures such as ResNet [15], DenseNet [16], and Transformer [17], and finally use ResNet as the backbone of feature extraction.

2.2. Phase correlation attention in the first-level Fusion

It is difficult to adequately determine the pulsar signal from single-mode data, and linear fusion in decision level between multimodal features cannot align "strong" features from different modality, such as in [7, 8]. To solve this problem, we consider that the phase link between the time- and frequency-phase maps can be used to fuse "strong" features from two maps to mutually reinforce "strong" signal features. Although these important phase positions change after covolutoin and pooling operations in ResNet, since the strengths of subband and subint are actually the same in phase, we can also backtrack through information such as signal strength and correlate the two by calculating the similarity between the intermediate features by

$$w(X_1, X_2) = f(E_1 - \left\| f(X_1^T) \cdot I - I^T \cdot f(X_2) \right\|), \quad (2)$$

where E_1 is an nxn matrix with all elements 1, I is an n-dimensional column vector with all elements 1, and we computes the absolute difference between the value at certain location (e.g., P1) after normalization of X_1 and the value at each location of X_2 to find the the location P_1 that is most similar to the location in X_2 by $\left\| f(X_1^T) \cdot I - I^T \cdot f(X_2) \right\|$, as shown in the correlation module of Fig. 2.

Since a greater weight should be assigned to the more similar positions, it needs to be inverted and normalized by subtracting it from E_1. Finally, we obtain the phase-associated attention $w(X_1, X_2)$ to integrate the features X_1 and X_2 from time-phase and frequency-phase respectively to obtain fused features X by

$$caf(X_1, X_2) = X_1 \cdot w(X_1, X_2) + X_2. \quad (3)$$

Since the two features X_1 and X_2 in a phase P_1 where a pulse appears, have been phase-correlated at this point, the fused features are enhanced.

2.3. Second-level fusion with DM curve

Dispersion curve (DM) is not a sufficient condition to determine whether a signal is a pulsar, but a waveform with a distinct wave peak is a necessary condition for the existence of a pulsar. Thus, we design a subnetwork based on the DM curve to extract the features, which can highlight the "peak" region.

The presence of unsmooth peak regions often indicates that a pulsar may occur at this period, so we need to quantify this condition by measuring the smoothness of the curve and the peak. Here, the frequency of the first-order derivative change of the curve is chosen as a measure of the unsmoothness as follows

$$smooth(i) = \left| sign(\triangle y(i+1)) - sign(\triangle y(i)) \right|, \quad (4)$$

where $\triangle y(i)$ is the first-order difference, $sign$ is the sign function, and the actual physical meaning of the formula is the number of first-order difference sign changes at that point. The segment peak is actually the maximum peak taken from different intervals. Then, we fuse the smoothness and peak features by

$$pf(X_{dm}) = \alpha_1 \cdot f(\Phi_P(X_{dm})) + \alpha_2 \cdot f(\Phi_S(X_{dm})), \quad (5)$$

where f refers to the softmax normalization function, $\Phi_P(X)$ refers to the calculation function of the segmented peak of the dispersion curve, and $\Phi_S(X)$ refers to the calculation function of the segmented smoothness of the dispersion curve. The weights α_1 and α_2 corresponding to the smoothness and peak are learnt by training data.

In the second layer of fusion, we integrate the peak features $caf(X_{dm})$ (3) extracted from the DM curves with the phase-correlation fusion features $pf(X_1, X_2)$ (5) obtained from the first layer of fusion to obtain the final discriminative information to improve the accuracy of the model by

$$score = f(caf(X_1, X_2)) \bigodot f\left(pf(X_{dm})\right), \quad (6)$$

where $\bigodot$ denotes if $f\left(pf(X_{dm})\right)$ is greater than a threshold such as 0.6, the result is $f(caf(X_1, X_2))$; otherwise, the result is the value obtained by multiplying them directly.

3. EXPERIMENT

3.1. Experimental setting

The dataset used in the following experiments is the FAST survey drift scan data, and the overall positive and negative samples of the dataset are extremely unbalanced. It can be available from https://github.com/dzuwhf/FAST_label_data. As discussed in Sect. 2.1, ResNet is chosen as a backbone of the subnetworks for time-phase and frequency-phase inputs. The learning rate is 0.001, the batch size is 32, the maximum number of iterations is 100, the loss function is cross-entropy and the optimization algorithm is stochastic gradient descent.

Table 1. Comparison of Single-layer vs double-layer fusion with phase-correlation attention.

Fusion mode	Model	Recall	Auc	Leak
Data (single)	CNN5	0.8988	0.8363	33
	ResNet18	0.9479	0.8603	17
	Transformer	0.9080	0.8366	30
Decision (single)	PICS	0.9755	0.9050	8
	PICS-v2	0.9816	0.9133	6
	SA+ResNet18	0.9877	0.9250	4
Ours (double)	CNN5	0.9785	0.9181	7
	ResNet18	0.9969	0.9306	1
	SA+ResNet18	**0.9969**	**0.9734**	**1**

Table 2. Comparison of Single modality with different attentions.

	Model	Recall	AUC	Leak
Subint	w/o	0.9724	0.8833	9
	SK	0.9816	0.9030	6
	CBAM	0.9847	0.9019	5
	SA	0.9877	**0.9078**	**4**
Subband	w/o	0.9847	0.8937	5
	SK	0.9755	0.8924	8
	CBAM	0.9785	0.8846	7
	SA	0.9939	**0.8991**	**2**
DM	Rule	1.0000	0.6123	0

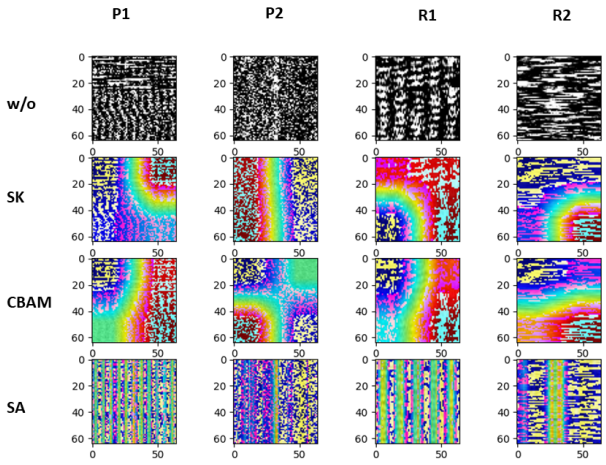

Fig. 3. **Visualization of different attention mechanisms for the subint images, where x-axis is phase, y-axis is time and the grey value of the graph indicates the intensity of the signal.** We visualize the attention weights of the network and overlay them with the original graph, which in turn indicates the region of attention of the feature extraction network. P1 and P2 denote pulsar signals, R1 and R2 denote non-pulsar signals, w/o denotes no attention, and SA denotes signal attention. From the SK attention [21, 22] on P2, one can see that similar signal features on phase can be obtained, but from SK and CBAM attentions [23] on P1, the highlighted areas have no pulse attention.

3.2. Experimental results

Single-level vs double-level fusion. In this paper, the proposed phase-correlation fusion networks with different backbones are compared with the fusion networks in data level [18, 19] and in decision level [7, 8, 20]. As shown in Tab. 1, the phase-correlation fusion is able to reinforce "strong" signals in the same phase between time-phase and frequency-phase images, and significantly outperforms the fusion models in data or decision levels.

Single modality with different attentions. By compared with multimodal inputs, the classification results by deep networks with different attentions are reported in Tab. 2 based on single modality, such time-phase (Subint) and frequency-phase (Subband) images. Note that hand-designed rule is applied for DM curve to filter out non-pulsar signals, where the recall is 100% but the precision is low. As shown in Tab. 2, one can see that signal attention can obtain significantly better recall and Auc on two single modalities than other attention mechanisms.

Furthermore, we can look at the impact of signal attention on feature extraction based on unimodal data. For instance as shown in Fig. 3 based on subint images, the pulsar data (e.g., P1 and P2) with signal attention (SA) has obvious pulsar features, while without (w/o) or with other image attentions such as SK [21, 22] and DBAM [23], although the features are "attended", no pulsar properties are captured. For non-pulsars such as R1 and R2, the suspected pulsed signals are captured from time-phase images by using SA. Although the conditions are satisfied from the subint images, pulsars can be excluded by the "peak" features of DM curves.

4. CONCLUSION

In the paper, a coupled deep fusion network has been proposed for identifying pulses based on radio astronomical signals.According to the characteristics of pulsar data, a two-stage deep fusion network fusion mechanism is designed. The first level of data fusion is achieved through a phase-correlated attention mechanism, by which pulses on the same phase reinforce each other on the time-phase and frequency phase maps that have been assigned to the signal attention mechanism. The second level filters out input signals that do not contain pulses. Afterwards, for signals with pulses after phase correlation enhancement signal fusion is performed on the decision level to obtain the final pulsar discrimination.

The proposed model evaluated on public FAST data, obtains the best recall and AUC compared to benchmark methods with different widely-used attentions.

5. REFERENCES

[1] H. Lin, X. Li, and Z. Luo, "Pulsars detection by machine learning with very few features," *Monthly Notices of the Royal Astronomical Society*, vol. 493, no. 2, pp. 1842–1854, 2020.

[2] K. Lee, K. Stovall, F. Jenet, J. Martinez, L. Dartez, A. Mata, G. Lunsford, S. Cohen, C. Biwer, M. Rohr *et al.*, "Peace: pulsar evaluation algorithm for candidate extraction–a software package for post-analysis processing of pulsar survey candidates," *Monthly Notices of the Royal Astronomical Society*, vol. 433, no. 1, pp. 688–694, 2013.

[3] M. Azhari, A. Abarda, A. Alaoui, B. Ettaki, and J. Zerouaoui, "Detection of pulsar candidates using bagging method," *Procedia Computer Science*, vol. 170, pp. 1096–1101, 2020.

[4] A. Singh and K. N. Pathak, "A machine learning-based approach towards the improvement of snr of pulsar signals," *arXiv preprint arXiv:2011.14388*, 2020.

[5] P. S. Chakraborty, "Detection of pulsars using machine learning algorithms–a study," *Artificial Intelligence for Internet of Things*, p. 210, 2019.

[6] H. Lin, X. Li, and Q. Zeng, "Pulsar candidate sifting using multi-input convolution neural networks," *The Astrophysical Journal*, vol. 899, no. 2, p. 104, 2020.

[7] W. W. Zhu, A. Berndsen, E. C. Madsen, M. Tan *et al.*, "Searching for pulsars using image pattern recognition," *The Astrophysical Journal*, vol. 781, no. 2, p. 117, 2014.

[8] H. Wang, W. Zhu, P. Guo, D. Li, S. Feng, Q. Yin, C. Miao, Z. Tao, Z. Pan, P. Wang *et al.*, "Pulsar candidate selection using ensemble networks for fast drift-scan survey," *Science China Physics, Mechanics & Astronomy*, vol. 62, no. 5, pp. 1–10, 2019.

[9] Q. Zeng, X. Li, and H. Lin, "Concat convolutional neural network for pulsar candidate selection," *Monthly Notices of the Royal Astronomical Society*, vol. 494, no. 3, pp. 3110–3119, 2020.

[10] V. Balakrishnan, D. Champion, E. Barr, M. Kramer, R. Sengar, and M. Bailes, "Pulsar candidate identification using semi-supervised generative adversarial networks," *Monthly Notices of the Royal Astronomical Society*, vol. 505, no. 1, pp. 1180–1194, 2021.

[11] P. Guo, F. Duan, P. Wang, Y. Yao, Q. Yin, and X. Xin, "Pulsar candidate identification with artificial intelligence techniques," *arXiv preprint arXiv:1711.10339*, 2017.

[12] L. Wang, J. Jin, Y. Jiang, and Y. Shen, "A method for weak pulsar signal detection combining the bispectrum and a deep convolutional neural network," *The Astrophysical Journal*, vol. 873, no. 1, p. 17, 2019.

[13] J. Holewik, G. Schaefer, and I. Korovin, "Imbalanced ensemble learning for enhanced pulsar identification," pp. 515–524, 2020.

[14] G. H. Pei Wang, Lei Zhang, "Wide-bandwidth drift-scan pulsar surveys of globular clusters:application to early science observations with fast," *Research in Astronomy and Astrophysics*, vol. 16, no. 10, pp. 13–22, 2016.

[15] K. He, X. Zhang, S. Ren, and J. Sun, "Deep residual learning for image recognition," *Proceedings of the IEEE conference on computer vision and pattern recognition*, pp. 770–778, 2016.

[16] G. Huang, Z. Liu, L. Van Der Maaten, and K. Q. Weinberger, "Densely connected convolutional networks," *Proceedings of the IEEE conference on computer vision and pattern recognition*, pp. 4700–4708, 2017.

[17] A. Vaswani, N. Shazeer, N. Parmar, J. Uszkoreit, L. Jones, A. N. Gomez, L. Kaiser, and I. Polosukhin, "Attention is all you need," *CoRR*, vol. abs/1706.03762, 2017.

[18] J. Gao, P. Li, Z. Chen, and J. Zhang, "A survey on deep learning for multimodal data fusion," *Neural Computation*, vol. 32, no. 5, pp. 829–864, 2020.

[19] P. Bota, C. Wang, A. Fred, and H. Silva, "Emotion assessment using feature fusion and decision fusion classification based on physiological data: Are we there yet?" *Sensors*, vol. 20, no. 17, p. 4723, 2020.

[20] C. Che, H. Wang, X. Ni, and R. Lin, "Hybrid multimodal fusion with deep learning for rolling bearing fault diagnosis," *Measurement*, vol. 173, p. 108655, 2021.

[21] X. Li, W. Wang, X. Hu, and J. Yang, "Selective kernel networks," *2019 IEEE/CVF Conference on Computer Vision and Pattern Recognition (CVPR)*, 2020.

[22] J. Hu, L. Shen, and G. Sun, "Squeeze-and-excitation networks," *Proceedings of the IEEE conference on computer vision and pattern recognition*, pp. 7132–7141, 2018.

[23] S. Woo, J. Park, J.-Y. Lee, and I. S. Kweon, "Cbam: Convolutional block attention module," *Proceedings of the European conference on computer vision (ECCV)*, pp. 3–19, 2018.